Simple and rapid characterization of novel large germline deletions in SDHB, SDHC and SDHD-related paraganglioma

Hoekstra, A.S.; Ende, B. van den; Julia, X.P.; Breemen, L. van; Scheurwater, K.; Tops, C.M.; ... ; Bayley, J.P.

CLINICAL GENETICS An International Journal of Genetics, Molecular and Personalized Medicine

Clin Genet 2017: 91: 536–544
Printed in Singapore. All rights reserved

CLINICAL GENETICS
doi: 10.1111/cge.12843

Original Article

Simple and rapid characterization of novel large germline deletions in *SDHB*, *SDHC* and *SDHD*-related paraganglioma

Hoekstra A.S., van den Ende B., Julià X.P., van Breemen L., Scheurwater K., Tops C.M., Malinoc A., Devilee P., Neumann H.P.H., Bayley J.-P. Simple and rapid characterization of novel large germline deletions in *SDHB*, *SDHC* and *SDHD*-related paraganglioma.
Clin Genet 2017: 91: 536–544. © 2016 The Authors. *Clinical Genetics* published by John Wiley & Sons A/S. Published by John Wiley & Sons Ltd., 2016

Germline mutations in genes encoding subunits of succinate dehydrogenase (SDH) are associated with hereditary paraganglioma and pheochromocytoma. Although most mutations in *SDHB*, *SDHC* and *SDHD* are intraexonic variants, large germline deletions may represent up to 10% of all variants but are rarely characterized at the DNA sequence level. Additional phenotypic effects resulting from deletions that affect neighboring genes are also not understood. We performed multiplex ligation-dependent probe amplification, followed by a simple long-range PCR 'chromosome walking' protocol to characterize breakpoints in 20 *SDH*x-linked paraganglioma-pheochromocytoma patients. Breakpoints were confirmed by conventional PCR and Sanger sequencing. Heterozygous germline deletions of up to 104 kb in size were identified in *SDHB*, *SDHC*, *SDHD* and flanking genes in 20 paraganglioma-pheochromocytoma patients. The exact breakpoint could be determined in 16 paraganglioma-pheochromocytoma patients of which 15 were novel deletions. In six patients proximal genes were also deleted, including *PADI2*, *MFAP2*, *ATP13A2* (*PARK9*), *CFAP126*, *TIMM8B* and *C11orf57*. These genes were either partially or completely deleted, but did not modify the phenotype. This study increases the number of known *SDH*x deletions by over 50% and demonstrates that a significant proportion of large gene deletions can be resolved at the nucleotide level using a simple and rapid method.

Conflict of interest

Nothing to declare.

A.S. Hoekstra[a], B. van den Ende[a], X.P. Julià[a], L. van Breemen[a], K. Scheurwater[a], C.M. Tops[b], A. Malinoc[c], P. Devilee[a,d], H.P.H. Neumann[c] and J.-P. Bayley[a]

[a]Department of Human Genetics, [b]Department of Clinical Genetics, Leiden University Medical Center, Leiden, The Netherlands, [c]Department of Nephrology, University Medical Center Freiburg, Freiburg, Germany, and [d]Department of Pathology, Leiden University Medical Center, Leiden, The Netherlands

Key words: breakpoint – deletion – paraganglioma – pheochromocytoma – SDHB – SDHC – SDHD – succinate dehydrogenase

Corresponding author: Jean-Pierre Bayley, Department of Human Genetics, Leiden University Medical Center, 2300 RC Leiden, The Netherlands.
Tel.: +31 71 5269512;
fax: +31 71 5268285;
e-mail: J.P.L.Bayley@lumc.nl
[PO BOX 9600]

Received 9 May 2016, revised and accepted for publication 27 July 2016

Head and neck paragangliomas (HN-PGLs) are generally benign, highly vascularized neuroendocrine tumors that are associated with the parasympathetic nervous system. HN-PGLs most frequently arise in the head and neck region as carotid body tumors at the carotid bifurcation. Extra-adrenal PGLs and pheochromocytomas (PCCs) are associated with the sympathetic nervous system, with extra-adrenal PGLs occurring in the sympathetic paraganglia anywhere from the neck to the pelvic floor, while PCCs originate in the chromaffin cells of the adrenal medulla (1). Extra-adrenal sympathetic PGLs may show an aggressive and metastatic growth pattern (2).

Germline mutations in the genes that encode succinate dehydrogenase (SDH), including *SDHA* (3), *SDHB* (4), *SDHC* (5), *SDHD* (6), and *SDHAF2* (7), are associated

with the development of familial PGL/PCC. SDH plays a central role in the tricarboxylic acid cycle, converting succinate to fumarate, while providing electrons for oxidative phosphorylation via the inner mitochondrial membrane. Despite the close functional relationship of the SDH proteins, mutations of subunit genes lead to clear differences in clinical phenotype. While *SDHD* and *SDHAF2* mutations predominantly result in head and neck PGLs, *SDHB* mutations are more closely associated with extra-adrenal PGL and metastatic disease (8, 9). *SDHA* and *SDHC* mutations are very rare and are currently associated with both PGL and PCC (10, 11).

A wide variety of *SDH* gene mutations have been described and listed in the SDH mutation database at http://chromium.liacs.nl/LOVD2/SDH/home.php (12), and over 400 variants are now included. The majority of mutations in the *SDH* genes are point mutations and small deletions, which are easily detected by direct sequencing. Large deletions are rarely detectable using this method, but the widespread adoption of multiplex ligation-dependent probe amplification (MLPA), and other methods has led to the identification of many large deletions (13–16). The SDH mutation database currently contains 31 large deletions, including some relatively common variants such as the *SDHB* Dutch founder deletion in exon 3 (17, 18). However, few deletions have been fully characterized and it is not known whether partial or complete deletion of additional genes has any phenotypic effect. In addition, mechanisms underlying deletion such as *Alu* repeat-mediated recombination, which is known to play a major role in germline deletions affecting *VHL* (19), have not yet been extensively explored in the *SDH* genes.

We collected samples from PGL/PCC patients who tested negative for point mutations by Sanger sequencing of the *SDH* genes. MLPA gene deletion analyses of *SDHB*, *SDHC* and *SDHD* in these patients led to the identification of 20 *SDH*-related gene deletions. The exact breakpoint could be determined in 16 PGL/PCC patients and the majority of these deletions were rapidly identified using a simple 'chromosome walking' long-range PCR method. Of the 15 novel deletions identified, six also affected neighboring genes. This study illustrates the ease-of-use of this long-range PCR method and suggests that it may be the most rapid and practical approach for further characterization of single or small number of deletions. However, this study also illustrates the drawbacks of this method in the analysis of complex or very large deletions (>100 kb).

Material and methods

Patients

DNA samples from 20 index paraganglioma/pheochromocytoma patients were obtained from the Albert-Ludwigs University, Freiburg. Genomic DNA was extracted using standard methods from EDTA-anticoagulated blood samples. Following initial Sanger sequencing and MLPA analysis at Albert-Ludwigs University, the samples were further analyzed at the Department of Human Genetics, Leiden University Medical Center. Informed consent was obtained for DNA testing according to protocols approved by ethics committee of the Albert-Ludwigs University, Freiburg. Clinical and genetic data for tumors included in the study are provided in Table S1 (Supporting information). All included patients were found to be negative for pathogenic mutations by sequencing.

MLPA

Screening for large deletions was carried out using the P226-B1 MLPA kit, following the manufacturer's protocol (MRC-Holland, Amsterdam, The Netherlands). This P226-B1 probemix contains probes for all exons of the *SDHB*, *SDHC* and *SDHD* genes. In addition, 10 reference probes are included in this probemix, detecting 10 different autosomal chromosomal locations.

Long-range PCR

Long-range PCR was carried out using the Takara LA Taq kit (Takara Bio Inc., Lucron Bioproducts, B.V., Gennep, The Netherlands) according to manufacturer's recommendations, except that the final volume was reduced to 20 µl. Approximately 30 ng of genomic DNA isolated from whole blood was used per reaction. The long-range PCR protocol was as follows: first an initial melting phase at 95°C for 3 min, followed by 35 cycles of 30 s at 95°C, 15 min at 68°C (20 min for fragments over 10 kb), and finally an extension phase for 10 min at 72°C. Primers were designed using the Primer3 program (http://frodo.wi.mit.edu/), with a left or right primer specified and subsequent primers selected using standard parameters (loosened when no primer was found). The primers used to determine the breakpoints of the 16 deletions identified in the *SDH* genes are described in Table S2. DNA sequences were downloaded from the UCSC genome browser using the pages *gene sorter*, *genomic sequence*, and *get genomic sequence near gene*, with the extent of appropriate upstream or downstream sequences specified, together with repeat masking. Primer3 allows the analysis of up to 200 kb of genomic sequence, so all primers required for a particular deletion analysis strategy were designed together. *Alu* sequences were analyzed using Repbase (Jurka, 2000) (http://www.girinst.org/repbase/index.html). PCR fragments spanning a deletion were characterized in detail by Sanger sequencing. Results from the sequenced PCR products were analyzed using either the Multalin program (http://multalin.toulouse.inra.fr/multalin/multalin.html) or the Blat program https://genome.ucsc.edu/cgi-bin/hgBlat. Deletion nomenclature follows HGVS guidelines.

Quantitative PCR

Broad mapping of the selected deletions was carried out by quantitative PCR of DNA using the iQ SYBR Green Supermix (Bio-Rad, CA) on a CFX96 Real-Time System (Bio-Rad). Bio-Rad CFX Manager 3.0 software was

used to analyze the data. Primers were designed using Primer3 software on repeat masked sequences (primer sequences available upon request). PCR reactions and quantification of PCR products were performed as previously described (20, 21). All measurements were carried out in triplicate. Ratios of 0.85–1.25 were accepted as diploid, while values of 0.35–0.70 were considered to be haploid, as described previously (19).

Results

MLPA analysis

MLPA analysis, which is based on the quantification of multiplexed amplified DNA fragments, allows the identification of large deletions. MLPA screening identified 10 cases with partial or complete germline deletions of *SDHB*, 4 cases with deletions of *SDHC* and 6 cases with deletions of *SDHD* (Table 1). Patients with *SDHB* deletions showed a variety of deletions in the proximal part of the gene including the *SDHB* promoter, exons 1 and 2 (patients 1, 2, 3 and 6), complete gene deletions (patients 4 and 5), and deletions affecting distal exons (patients 8, 9 and 10). A previously described Dutch founder deletion affecting exon 3 of the *SDHB* gene was identified in one patient (patient 7) (17).

Of the four patients with *SDHC*-related deletions, three had deletions that extended beyond the boundaries of the gene, including two patients with deletions in exons 4, 5 and 6 (patients 11 and 12), and patient 14 with a deletion of exons 5 and 6 (Table 1). Only patient 13 showed a deletion confined to the internal exons 3 and 4.

Of the six patients with deletions in *SDHD*, five had deletions that affected extragenic regions, including distal deletions affecting exons 3 and 4 (patient 15 and 20), deletions of the *SDHD* promoter and proximal exons (patients 16 and 17) and a complete gene deletion (patient 18). One patient appeared to have an internal deletion confined to exon 3 of *SDHD* (patient 19).

Table 1. Multiplex ligation-dependent probe amplification (MLPA) results of 20 *SDH*-related patients

Patient number	Gene mutation	Description MLPA
1	*SDHB*	Del promoter + exon 1
2	*SDHB*	Del promoter + exon 1
3	*SDHB*	Del promoter + exon 1 + 2
4	*SDHB*	Del promoter + exon 1-8
5	*SDHB*	Del promoter + exon 1-8
6	*SDHB*	Del exon 1
7	*SDHB*	Del exon 3
8	*SDHB*	Del exon 6 + 7
9	*SDHB*	Del exon 6–8
10	*SDHB*	Del exon 2–8
11	*SDHC*	Del exon 4–6
12	*SDHC*	Del exon 4–6
13	*SDHC*	Del exon 3 + 4
14	*SDHC*	Del exon 5 + 6
15	*SDHD*	Del exon 4
16	*SDHD*	Del promoter + exon 1
17	*SDHD*	Del promoter + exon 1–3
18	*SDHD*	Del promoter + exon 1–4
19	*SDHD*	Del exon 3
20	*SDHD*	Del exon 3 + 4

Long-range 'chromosome walking' PCR

We used long-range PCR to refine deleted regions and, in some cases, to immediately identify exact breakpoints. Long-range PCR is conventionally used as a secondary method to narrow regions around deletions that have been located approximately by other methods such as qPCR or microsatellite mapping. In a previous publication we briefly described exclusive use of long-range PCR in the rapid mapping of the breakpoints of four *SDH* gene deletions (13). Here we wished to further explore the practicality of using this approach as a primary method of breakpoint identification. Forward or reverse primers were designed in undeleted regions of the *SDH* genes when known, with strategies for individual deletions developed based on the known location of deleted and retained regions as defined by MLPA. For example, in the case of a proximal deletion extending for an unknown distance upstream of a gene, several reverse primers are designed in a retained exon and into the possibly retained proximal intron region (Fig. 1a). Forward primers are concurrently designed at increasing distances beyond the region known to be deleted, with steps of around 5 kb, depending on the location of masked repeat regions in the gene sequence. Following long-range PCR, amplified products are analyzed by gel electrophoresis and compared to theoretical products from the wild type allele and possible deletion alleles. The staggered design of primers pairs (R1 + F1, R1 + F2, R1 + F3, etc.) will in some cases produce a ladder effect on an agarose gel that immediately suggests the presence of a deletion. In other cases, a single dominant product of the correct size will suggest a specific PCR product. Suspected positive PCR products must be confirmed by Sanger sequencing (Fig. 1b). The breakpoint can then be directly sequenced from such deletion junction-containing fragments or further refined by conventional PCR and sequencing.

Thirteen of 20 deletions were rapidly identified using this 'chromosome walking' long-range PCR approach. Ranging from 2.5 kb up to 44 kb, 10 deletions included extragenic regions. A total of 288 PCR reactions were required to identify the breakpoints of 13 deletions, representing an average of 22 PCR reactions per deletion. Even using the relatively basic and low-throughput approach of 96-well PCR followed by gel electrophoresis, little more than three PCR plates were required to identify these deletion breakpoints. In some cases where products were too large for convenient sequencing across a breakpoint or mononucleotide repeats hindered sequencing, additional primers were designed to simplify Sanger sequencing.

By contrast, an additional 629 PCR reactions failed to identify the seven unresolved deletion breakpoints (approximately 90 per deletion). Deletions encompassing an entire gene were particularly problematic, because

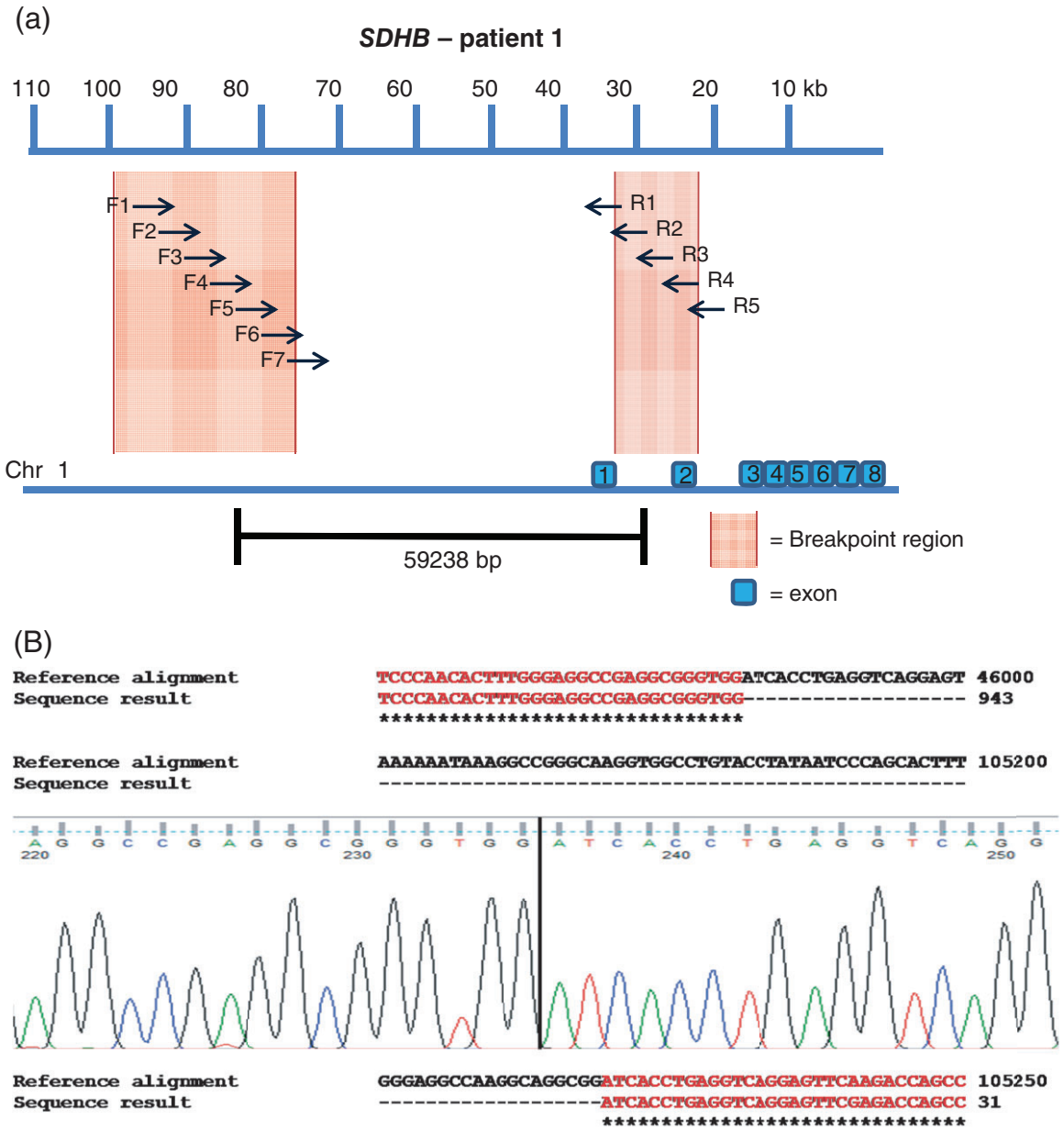

Fig. 1. Long-range PCR mapping strategy to identify the breakpoints of the deletion. (**a**) Patient 1. F and R indicate approximate positions of the forward and reverse primers used for *SDHB*. Genomic DNA is represented by horizontal lines with exons as blue boxes. The size of the deletion was 59,238 bp. (**b**) The breakpoint is identified by sequencing with the black line indicating the breakpoint. Alignment of the *SDHB* gene (red) shows the continuous region of mismatch and the breakpoints (black).

in the absence of an anchoring gene sequence the number of forward and reverse primer combinations expands rapidly and results in significant numbers of false positive PCR products that have to be further analyzed. Extended analysis can also lead to the depletion of DNA samples that are only available in limited quantities.

Mapping of deletions by qPCR

The seven deletions (patients 1, 4, 5, 13, 14, 15, 18) that could not be resolved by long-range PCR analyses were subjected to broad mapping by SYBR Green qPCR (20). Primers were designed to amplify 100–300 bp DNA fragments of the genomic sequence of the *SDHB*, *SDHC* and *SDHD* genes, using steps of around 8 kb between primer sets and including 100 kb upstream and 100 kb downstream of the coding regions where appropriate. Amplicons of patient DNA with an unresolved deletion were compared to amplicons derived from DNA lacking an *SDH* gene deletion. Relative ratios of 0.85–1.25 were considered to be diploid, while values of 0.35–0.70 were taken as indicators of a haploid genome region.

The deletion breakpoint for patient 1 (deletion of *SDHB* promoter and exon 1) was narrowed by qPCR

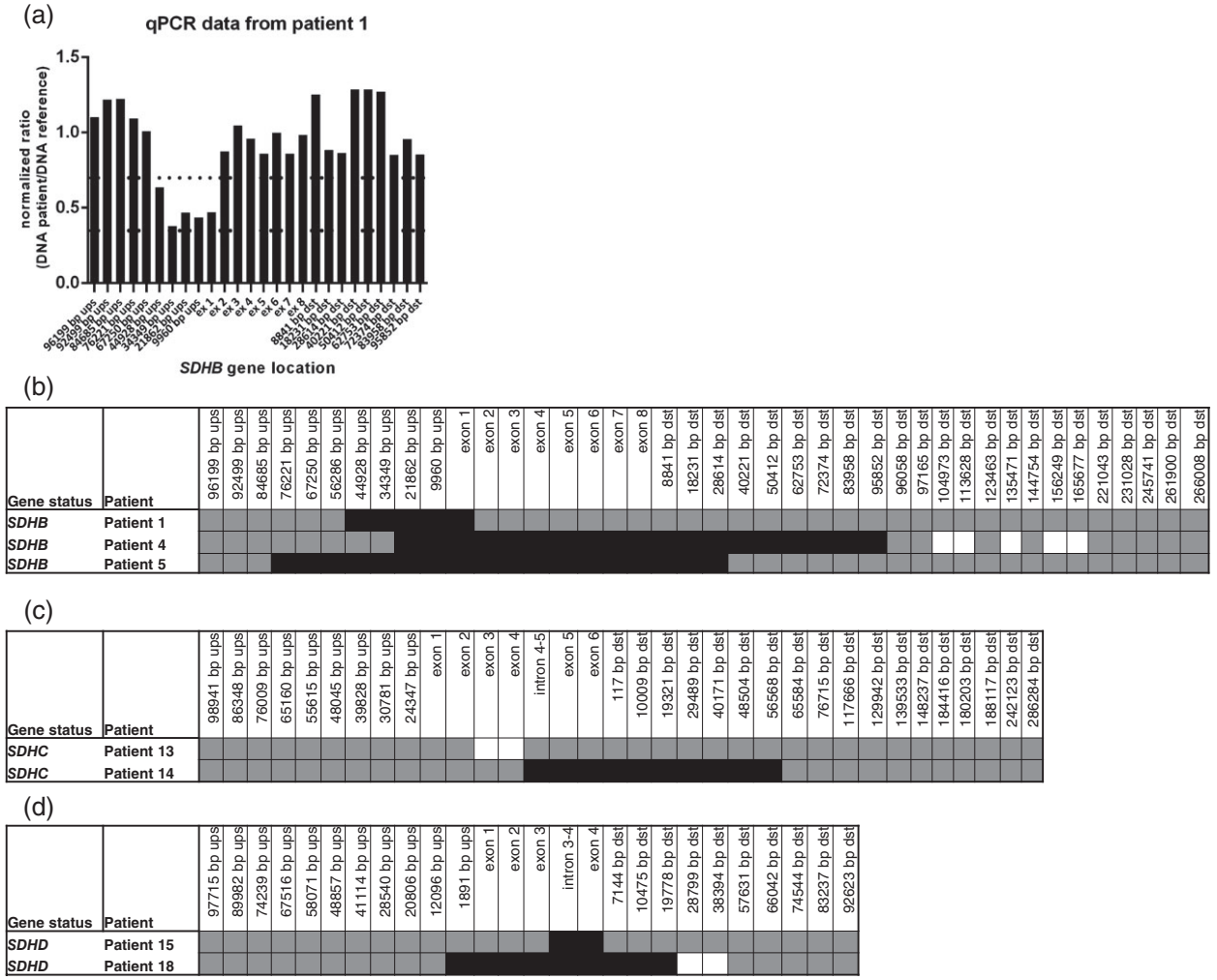

Fig. 2. Result of fine mapping of deletions by qPCR. Primers were designed to amplify 100–300 bp DNA fragments of the genomic sequence of the *SDH* gene, using steps of around 10 kb between primer sets and including 100 kb upstream and 100 kb downstream of the coding regions. (**a**) Normalized qPCR result of patient 1, with the dashed line indicating the deleted region based on ratio values of 0.35–0.70. (**b**) Primers 96 kb upstream and 266 kb downstream of *SDHB* are used for qPCR. (**c**) Primers 98 kb upstream and 286 kb downstream of *SDHC* are used for qPCR. (**d**) Primers 97 kb upstream and 92 kb downstream of *SDHD* are used for qPCR. Black blocks represents the deleted region based on ratio values of 0.35–0.70. Gray blocks represents the retained region based on ratio values of 0.85–1.25. Inconclusive results are indicated by white blocks based on ratio values of 0.75–0.85.

analysis to a region 44 kb upstream of *SDHB* (Fig. 2a). The breakpoints for patient 4 were mapped to regions 21 kb upstream and 95 kb downstream of *SDHB*. However, downstream qPCR results were variable, with ratios of 0.70–0.90 in the region 96 kb to 165 kb of *SDHB*. Breakpoints for patient 5 were mapped to areas 76 kb upstream and 28 kb downstream of *SDHB* (Fig. 2a). A deletion in *SDHC* exons 3 and 4 (patient 13) determined by MLPA analysis gave inconclusive qPCR results in this region with ratios of 0.75–0.85 (Fig. 2b). The deletion breakpoint for patient 14 (deletion of *SDHC* exons 5 and 6) was narrowed to a 56 kb region downstream of *SDHC* (Fig. 2b).

Patient 15 carried a deletion of exon 4 of the *SDHD* gene that extended only slightly beyond the end of gene (Fig. 2c). The breakpoints of patient 18, with a complete *SDHD* gene deletion, were narrowed by qPCR mapping to regions 2 kb upstream and 38 kb downstream of *SDHD* (Fig. 2c). However, the downstream region was uncertain, due to borderline ratios of 0.75–0.85.

Breakpoint characterization

Following the further refinement of deleted regions by qPCR, we again applied the long-range PCR approach described above to identify exact breakpoints. Exact positions of the breakpoints could be determined in further three patients (patients 1, 5, 15). Of the four unresolved patients, three showed poor results suggesting low-quality DNA (patients 4, 13 and 14), and one could not be resolved due to exhaustion of available DNA (patient 18). All results are listed in Table 2, which also provides information on neighboring genes affected by deletions. We have included schematic figures of all deletions and the location of the breakpoints identified in *SDHB* (Fig. S1), *SDHC* (Fig. S2), and *SDHD* carriers

Table 2. Exactly defined breakpoints and deletion sizes in 16 *SDH*-linked patients

Patient number	Description MLPA information	Size deletion (bp)	HGVS description	Associated repeats/ other features	Other affected genes
1	*SDHB* del promoter + exon 1	59238	NG_012340.1 (NM_003000.2): c.1-54121_73-4014del	5′ *Alu*Sq 3′ *Alu*Sq	*PADI2* all but first exon deleted
2	*SDHB* del promoter + exon 1	3019	NG_012340.1 (NM_003000.2): c.1-516_72 + 333del	None	None
3	*SDHB* del promoter + exon 1 + 2	28199	NG_012340.1 (NM_003000.2): c.1-8570_201-1396del	5′ *Alu*Sz 3′ *Alu*Sz	None
4	*SDHB* del promoter + exon 1–8	?	NG_012340.1 (NM_003000.2): c.1 + 1_*1_?del		
5	*SDHB* del promoter + exon 1-8	103903	NG_012340.1 (NM_003000.2): c.1-24771_*1 + 43992del	5′ *Alu*Jb	*MFAP2* complete deletion, *ATP13A2* complete deletion, *PADI2* last five exons deleted
6	*SDHB* del exon 1	2530	NG_012340.1 (NM_003000.2): c.1-584_72 + 1872del	5′ *Alu*Sq 3′ *Alu*Sq	None
7	*SDHB* del exon 3	7905	NG_012340.1 (NM_003000.2): c.201-4429_287-933del	5′ *Alu*S	None
8	*SDHB* del exon 6 + 7	8240	NG_012340.1 (NM_003000.2): c.540 + 266_766-341 del.ins17	17 bp insertion	None
9	*SDHB* del exon 6–8	8182	NG_012340.1 (NM_003000.2): c.541-1549_*1 + 1692del.ins6	6 bp insertion	None
10	*SDHB* del exon 2–8	33973	NG_012340.1 (NM_003000.2):c.72 + 2025_*1 + 931del	5′ *Alu*Sx1 3′ *Alu*Sx1	None
11	*SDHC* del exon 4–6	44028	NG_012767.1 (NM_001278172.1): c.179 + 1931_*1 + 12026del	5′ MLT1-int	*CFAP126* complete deletion
12	*SDHC* del exon 4–6	44028	NG_012767.1 (NM_001278172.1): c.179 + 1931_*1 + 12026del	5′ MLT1-int	*CFAP126* complete deletion
13	*SDHC* del exon 3 + 4	?	NG_012767.1 (NM_001278172.1): c.77-?_c.179 + ?del		
14	*SDHC* del exon 5 + 6	?	NG_012767.1 (NM_001278172.1): c.241 + *1_?del		
15	*SDHD* del exon 4	4944	NG_012337.3 (NM_001276506.1): c.315-726_*1 + 4052del	5′ *Alu*Sq	None
16	*SDHD* del promoter + exon 1	2409	NG_012337.3 (NM_001276506.1): c.1-1949_52 + 408del	None	*TIMM8B* (*DDP2*) complete deletion
17	*SDHD* del promoter + exon 1–3	10636	NG_012337.3 (NM_001276506.1): c.1-2651_315del	None	*TIMM8B* (*DDP2*) complete deletion, *C11orf57* 3′UTR partially deleted
18	*SDHD* del promoter + exon 1–4	?	NG_012337.3 (NM_001276506.1): c.1 + *1_?del		
19	*SDHD* del exon 3	2640	NG_012337.3 (NM_001276506.1): c.169 + 168_314 + 177del	None	None
20	*SDHD* del exon 3 + 4	6571	NG_012337.3 (NM_001276506.1): c.170-80_*1 + 895del.ins133	133 bp insertion	None

CFAP126, cilia and flagella associated protein 126; MFAP2, microfibrillar-associated protein 2; MLT1, mammalian long terminal repeat (LTR)-transposon 1; PADI2, peptidyl arginine deiminase 2; SDH, succinate dehydrogenase; TIMM8B (DDP2), mitochondrial import inner membrane translocase subunit tim8 B.

(Fig. S3). Of the 16 deletions, 13 were simple deletions and 3 were deletions-insertions, including a 17 bp insertion (patient 8), a 6 bp insertion (patient 9), and an insertion of 133 bp in patient 20 that was identified as an *Alu*S repeat.

We also analyzed the breakpoint regions using Repbase (22) to determine whether *Alu–Alu* recombination is an underlying mechanism driving deletion in the *SDH* genes. Single deletion breakpoints were located in *Alu* repeats (patients 5, 7, 15) or in a mammalian long terminal repeat (LTR)-transposon 1 (MLT1) element (patients 11, 12) in the *SDHD* and *SDHC* genes providing no evidence for an influence of repeat sequences. Evidence for *Alu–Alu* recombination-mediated deletion was found for four *SDHB* gene deletions (patients 1, 3, 6, 7).

Proximal genes

Several of the identified *SDH* gene deletions also affected neighboring genes. Patient 1 showed a deletion in the *SDHB* promoter together with exon 1 that also extended to include exons 2–16 of *PADI2* (Peptidyl Arginine Deiminase 2) upstream of *SDHB*. In addition to complete gene deletion of *SDHB* in patient 5, upstream of *SDHB* exons 11–16 of *PADI2* were lost and downstream the *MFAP2* (Microfibrillar-Associated Protein 2) and *ATP13A2* (*PARK9*) genes were entirely deleted. Mutations in *ATP13A2*/*PARK9* have been linked to genetic forms of early onset Parkinsonism (23). Patients 11 and 12 showed, in addition to deletion of *SDHC* exons 4–6, complete deletion of *CFAP126* (Cilia And Flagella Associated Protein 126) (Table 2). Complete gene deletion of *TIMM8B* (Mitochondrial import inner membrane translocase subunit Tim8 B) upstream of *SDHD* was found in patient 16. Patient 17 also showed deletion of the entire *TIMM8B* gene, in addition to partial deletion of *C11orf57*, upstream of *SDHD*.

Discussion

In this study, we characterized germline deletions of the *SDH* genes and flanking genes, identifying precise deletion breakpoints in 16 patients and deletions of up to 104 kb in size. The average size of a deletion was 23 kb. This study underlines the fact that clinically relevant deletions may encompass neighboring genes, with the potential to modify phenotype. Six of the deletions affected genes proximal to *SDH*. Deletions affecting neighboring genes may influence phenotypes, as apparent in the case of the *VHL* gene in which deletion of the actin regulator gene *BRK1* together with the *VHL* gene reduces risk for renal cell carcinoma, kidney cysts and retinal angiomas (19, 24, 25). Patient 1, with a deletion of the *SDHB* gene promoter and exon 1, also showed a deletion of exons 2–16 of *PADI2*. PAD enzymes convert protein arginine to citrulline, and citrullination has been associated with autoimmune responses such as those seen in rheumatoid arthritis (RA) (26). Certain polymorphisms of the *PADI2* gene are also associated with RA (27). No additional phenotype is currently recognized in patient 1. In addition to complete gene deletion of *SDHB*, patient 5 was also affected by deletion of exons 11–16 of *PADI2* and complete deletion of the genes *MFAP2* and *ATP13A2* (PARK9). *MFAP2* is an antigen of elastin-associated microfibrils and may affect hematopoiesis (28). *Mfap2*$^{-/-}$ mice show bone abnormalities, hematopoietic changes, increased fat deposition, diabetes, compromised wound repair, and bleeding diathesis (29). However, no human mutations in *MFAP2* are currently known and heterozygous deletion of *MFAP2* in this patient did not lead to an additional phenotype. *ATP13A2* (PARK9) is involved in the pathogenesis of movement disorders and a heterozygous *ATP13A2* gene frameshift mutation has been reported to cause juvenile Parkinsonism, a disease with an onset under 21 years of age (23). Patient 5 had complete loss of one *ATP13A2* allele, but no additional clinical features associated with Parkinsonism. A large *ATP13A2* deletion has never been reported before in the literature. This deletion may not result in a phenotype because it currently appears that mutations with a relatively mild structural effect result in misfolded proteins that are the actual cause of symptoms, probably acting as dominant negative proteins (30). If this patient had a Parkinson-like phenotype it would be the very first report of such a pathogenic mutation in this disease, and would require a re-think of pathogenic mechanisms.

Two patients with a deletion in exons 4–6 of *SDHC* (patient 11 and 12) also showed complete deletion of the *CFAP126* gene. This gene might play a role in Charcot–Marie–Tooth disease, however no mutations in *CFAP126* have been reported to date. In two other patients, genes proximal to *SDHD* were also affected by the deletion of *TIMM8B* (patients 16 and 17) and *C11orf57* (patient 17). Little is known about the function of these genes but heterozygous deletions are not known to result in an additional phenotype (13). Although we did not observe any clinical repercussions that can be attributed to deletions in these neighboring genes, some patients may be too young for a full phenotype to be manifested.

Of the 32 sequenced breakpoints, 13 (40%) were located in repeats, of which 11 (34% of total) were *Alu* elements. Most breakpoints located in *Alu* elements were identified in *SDHB*-related cases (10/18, 55%). In four *SDHB*-related cases there was evidence for *Alu–Alu* recombination-mediated deletion and analysis of the genomic structure of the *SDHB* gene revealed a high density of *Alu* repeats (44 elements that represent 31% of the sequence). A high density of *Alu* elements is likely to contribute to homologous *Alu*-mediated recombination, as shown for *VHL* mutant PCCs where most large *VHL* gene deletions are caused by recombination events driven by *Alu* repeat sequences (19). The *VHL* locus sequence shows a very high *Alu* density of 49%, this may predispose the *VHL* gene to a high frequency of *Alu*-mediated deletions, in contrast to the *SDH* genes (mean *Alu* density of 29%). Our results suggest that *Alu*-mediated recombination does not play a major role in the deletion of *SDH* genes, since only 34% of all *SDH* deletions were located in *Alu* elements compared to 90% of *VHL* deletions (19).

This study also illustrates the practicality of a long-range 'chromosome walking' PCR strategy in the rapid and efficient mapping of deletion breakpoints. Although large deletions may represent up to 10% of all *SDH*x mutations, on a per center basis they are relatively rare and most centers will find few large deletions. At this point further mapping becomes problematic in terms of return on time invested. On the one hand, benefits of precise breakpoint mapping include exact identification of a variant, which facilitates family studies and the identification of founder mutations. The sequence-related mechanisms underlying large deletions can only be elucidated by breakpoint mapping. Furthermore, as so few deletions have been mapped in detail, we currently know little about possible additional phenotypes or phenotypic modification. On the other hand, drawbacks include the time required to map breakpoints, the expense and relative technical complexity of typical first-line methods such as qPCR, and the uncertainty surrounding the relevance and meaning of results. Our experience in this study suggests that any lab with a basic competence in molecular biology could rapidly map the majority of gene deletion breakpoints using standard equipment, and with personnel with limited experience. We suggest that while all deletions could be considered targets for long-range 'chromosome walking' PCR, this technique is at its most efficient when used to tackle deletions that show retention of some part of a gene. In practical terms, using this technique to analyze more than 100 kb flanking either side of a gene yields diminishing returns and other approaches such as qPCR or microsatellite mapping should perhaps be considered. Limitations of the chromosome walking approach include the lack of a positive control in PCR reactions, the possibility of false negative findings due to primers that produce PCR deletion products too large for efficient amplification (>10–12 kb) and the numerous off-target PCR products produced when primers are not consumed in the amplification of bona fide products.

In several cases, we used qPCR for further mapping of large deletions in the *SDH* genes. When successful, upstream or downstream gene regions can be very rapidly narrowed. However, this approach is relatively costly, time-consuming, difficult to interpret, and requires close supervision of inexperienced personnel. Our results were not always conclusive, possibly due to the variable quality of certain DNA samples, the inexperience of staff and to the intrinsically wider variability of this quantitative technique. As newer technologies, such as digital PCR, targeted arrays, targeted panel sequencing, and next-generation sequencing, are increasingly being used for routine clinical screening, and the costs for genome sequencing decreases, these techniques could be used in the future to detect copy-number changes (31).

In conclusion, we identified 15 novel deletions, increasing the number of reported *SDH*x deletions to 46. The majority of deletions found in this study fell within the reach of our 'chromosome walking' approach. In several cases the initial characterization and confirmation of a deletion could be completed in a single long-range PCR experiment, followed directly by Sanger sequencing using the same primers. We hope that this method will provide a low threshold approach for labs facing the dilemma of whether to invest time and resources in the full characterization of deletions. Only by fully characterizing deletions and monitoring patients for possible additional phenotypes can we determine whether specific *SDH*x deletions and/or loss of neighboring genes have phenotypic consequences. Improved understanding of the function of deleted neighboring genes may allow new insights into subtle clinical effects.

Supporting Information

Additional supporting information may be found in the online version of this article at the publisher's web-site.

Acknowledgements

We thank the clinicians and patients involved for their cooperation. This work was supported by the Dutch Cancer Society (Grant 2011–5025 to JPB/PD).

Reference

1. Petri BJ, van Eijck CH, de Herder WW, Wagner A, de Krijger RR. Phaeochromocytomas and sympathetic paragangliomas. Br J Surg 2009: 96 (12): 1381–1392.
2. Benn DE, Gimenez-Roqueplo AP, Reilly JR et al. Clinical presentation and penetrance of pheochromocytoma/paraganglioma syndromes. J Clin Endocrinol Metab 2006: 91 (3): 827–836.
3. Burnichon N, Briere JJ, Libe R et al. SDHA is a tumor suppressor gene causing paraganglioma. Hum Mol Genet 2010: 19 (15): 3011–3020.
4. Astuti D, Latif F, Dallol A et al. Gene mutations in the succinate dehydrogenase subunit SDHB cause susceptibility to familial pheochromocytoma and to familial paraganglioma. Am J Hum Genet 2001 July: 69 (1): 49–54.
5. Niemann S, Muller U. Mutations in SDHC cause autosomal dominant paraganglioma, type 3. Nat Genet 2000: 26 (3): 268–270.
6. Baysal BE, Ferrell RE, Willett-Brozick JE et al. Mutations in SDHD, a mitochondrial complex II gene, in hereditary paraganglioma. Science 2004: 287 (5454): 848–851.
7. Hao HX, Khalimonchuk O, Schraders M et al. SDH5, a gene required for flavination of succinate dehydrogenase, is mutated in paraganglioma. Science 2009: 325 (5944): 1139–1142.
8. Neumann HP, Pawlu C, Peczkowska M et al. Distinct clinical features of paraganglioma syndromes associated with SDHB and SDHD gene mutations. JAMA 2004: 292 (8): 943–951.
9. Ricketts CJ, Forman JR, Rattenberry E et al. Tumor risks and genotype-phenotype-proteotype analysis in 358 patients with germline mutations in SDHB and SDHD. Hum Mutat 2010: 31 (1): 41–51.
10. Benn DE, Robinson BG, Clifton-Bligh RJ. 15 years of paraganglioma: clinical manifestations of paraganglioma syndromes types 1–5. Endocr Relat Cancer 2015: 22 (4): T91–T103.
11. Peczkowska M, Cascon A, Prejbisz A et al. Extra-adrenal and adrenal pheochromocytomas associated with a germline SDHC mutation. Nat Clin Pract Endocrinol Metab 2008: 4 (2): 111–115.
12. Bayley JP, Devilee P, Taschner PE. The SDH mutation database: an online resource for succinate dehydrogenase sequence variants involved in pheochromocytoma, paraganglioma and mitochondrial complex II deficiency. BMC Med Genet 2005: 6: 39.
13. Bayley JP, Weiss MM, Grimbergen A et al. Molecular characterization of novel germline deletions affecting SDHD and SDHC in pheochromocytoma and paraganglioma patients. Endocr Relat Cancer 2009: 16 (3): 929–937.
14. Burnichon N, Rohmer V, Amar L et al. The succinate dehydrogenase genetic testing in a large prospective series of patients with paragangliomas. J Clin Endocrinol Metab 2009: 94 (8): 2817–2827.
15. Cascon A, Montero-Conde C, Ruiz-Llorente S et al. Gross SDHB deletions in patients with paraganglioma detected by multiplex PCR: a possible hot spot? Genes Chromosomes Cancer 2006: 45 (3): 213–219.

16. McWhinney SR, Pilarski RT, Forrester SR et al. Large germline deletions of mitochondrial complex II subunits SDHB and SDHD in hereditary paraganglioma. J Clin Endocrinol Metab 2004: 89 (11): 5694–5699.
17. Bayley JP, Grimbergen AE, van Bunderen PA et al. The first Dutch SDHB founder deletion in paraganglioma-pheochromocytoma patients. BMC Med Genet 2009: 10: 34.
18. Hensen EF, van DN, Jansen JC et al. High prevalence of founder mutations of the succinate dehydrogenase genes in the Netherlands. Clin Genet 2012: 81 (3): 284–288.
19. Franke G, Bausch B, Hoffmann MM et al. Alu-Alu recombination underlies the vast majority of large VHL germline deletions: molecular characterization and genotype-phenotype correlations in VHL patients. Hum Mutat 2009: 30 (5): 776–786.
20. Boehm D, Herold S, Kuechler A, Liehr T, Laccone F. Rapid detection of subtelomeric deletion/duplication by novel real-time quantitative PCR using SYBR-green dye. Hum Mutat 2004: 23 (4): 368–378.
21. Borozdin W, Boehm D, Leipoldt M et al. SALL4 deletions are a common cause of Okihiro and acro-renal-ocular syndromes and confirm haploinsufficiency as the pathogenic mechanism. J Med Genet 2004: 41 (9): e113.
22. Jurka J. Repbase update: a database and an electronic journal of repetitive elements. Trends Genet 2000: 16 (9): 418–420.
23. Fong CY, Rolfs A, Schwarzbraun T, Klein C, O'Callaghan FJ. Juvenile parkinsonism associated with heterozygous frameshift ATP13A2 gene mutation. Eur J Paediatr Neurol 2011: 15 (3): 271–275.
24. Cascon A, Escobar B, Montero-Conde C et al. Loss of the actin regulator HSPC300 results in clear cell renal cell carcinoma protection in Von Hippel-Lindau patients. Hum Mutat 2007: 28 (6): 613–621.
25. Maranchie JK, Afonso A, Albert PS et al. Solid renal tumor severity in von Hippel Lindau disease is related to germline deletion length and location. Hum Mutat 2004: 23 (1): 40–46.
26. Foulquier C, Sebbag M, Clavel C et al. Peptidyl arginine deiminase type 2 (PAD-2) and PAD-4 but not PAD-1, PAD-3, and PAD-6 are expressed in rheumatoid arthritis synovium in close association with tissue inflammation. Arthritis Rheum 2007: 56 (11): 3541–3553.
27. Chang X, Xia Y, Pan J, Meng Q, Zhao Y, Yan X. PADI2 is significantly associated with rheumatoid arthritis. PLoS One 2013: 8 (12): e81259.
28. Combs MD, Knutsen RH, Broekelmann TJ et al. Microfibril-associated glycoprotein 2 (MAGP2) loss of function has pleiotropic effects in vivo. J Biol Chem 2013: 288 (40): 28869–28880.
29. Weinbaum JS, Broekelmann TJ, Pierce RA et al. Deficiency in microfibril-associated glycoprotein-1 leads to complex phenotypes in multiple organ systems. J Biol Chem 2008: 283 (37): 25533–25543.
30. Park JS, Blair NF, Sue CM. The role of ATP13A2 in Parkinson's disease: clinical phenotypes and molecular mechanisms. Mov Disord 2015: 30 (6): 770–779.
31. Smith MJ, Urquhart JE, Harkness EF et al. The contribution of whole gene deletions and large rearrangements to the mutation spectrum in inherited tumor predisposing syndromes. Hum Mutat 2016: 37 (3): 250–256.